doi:10.3788/gzxb20174606.0616004

基于石墨烯超材料表面等离子体激元共振的增强太赫兹调制

王梦奇,孙丹丹,任兆玉

(西北大学 光子学与光子技术研究所,西安 710069)

摘 要:基于表面等离子体共振原理,采用石墨烯超材料设计了开口环结构,用于调制太赫兹波.增加石墨烯的费米能级,改变开口环的开口距离,叠加多层石墨烯以增强石墨烯超材料的共振强度,进而增强太赫兹波调制,调制频率范围包括低频段和高频段.由于石墨烯费米能级的可调谐性,单层结构在高低两个频段的调制深度分别为 81%和 68%,多层结构在高低两个频段的调制深度分别增加到 93%和 95%,为动态调制提供了可能.该设计为调制器、吸收体等太赫兹器件的设计提供了指导和借鉴.

关键词:超材料;等离子体;共振;调制深度;石墨烯

中图分类号:O441 **文献标识码**:A **文章编号**:1004-4213(2017)06-0616004-7

Enhanced Terahertz Modulation by Harvesting the Surface-plasmon-polariton Modes Based on Graphene Metamaterial

WANG Meng-qi, SUN Dan-dan, REN Zhao-yu

(*Institute of Photonics & Photon-Technology, Northwest University, Xi'an* 710069, *China*)

Abstract: Graphene-based Split Ring Resonator (SRR) metamaterial is proposed with capacity of modulating transmitted THz waves based on the principle of surface-plasmon-polariton. The resonant strengths of plasmonic modes can be significantly enhanced by increasing the Fermi level of graphene, changing the gap distance of SRR or by stacking graphene layers, thus high modulation depth is achieved in both higher frequency region and lower frequency region. Modulation depth of 81% and 68% are achieved in the two regions, which can be further enhanced to 93% and 95%, provides a dynamical modulation based on controllable Fermi level of graphene. This graphene-based design paves the way forthe design of THz applications, such as modulators and absorbers.

Key words: Metamaterial; Plasmonic; Resnonace; Modulation depth; Graphene

OCIS Codes: 160.3918; 250.5403; 260.5740

0 Introduction

Graphene is a promisingcandidate in many fields due to its unique mechanical, thermal, electronic and optical properties[1-3]. It has been proved to have many optoelectronic applications such as modulators, absorbers, detectors and polarizers[4-7]. Especially, graphene has shown potential to manipulate terahertz (THz) waves mainly due to the controllable interaction between THz waves and graphene by turning its Fermi level as well as carrier concentration via physical and chemical methods[8-9], which can be used in the

Foundation item: The National Natural Science Foundation of China (Nos. 61275105, 61606160), the International Cooperative Program (No. 201410780)

First author: WANG Meng-qi (1992—), male, M. S. degree candidate, mainly focuses on graphene based optical modulator. Email: mq-wang@foxmail.com

Supervisor(Contact author): REN Zhao-yu (1958—), female, professor, Ph. D. degree, mainly focuses on two-dimensional nano-material. Email: rzy@nwu

Received: Dec. 26, 2016; **Accepted**: Feb. 27, 2017

design of THz devices[10-11]. However, the interaction between graphene and THz waves is not strong enough for practical THz applications due to its nonresonant Drude-like behavior[12-13]. Artificially constructed material (metamaterial) can be introduced for this purpose. The plasmonic resonances on metamaterials excited by incident light can be possibly tailored via their structure and size[14], which play a vital role in modulation and manipulation of electromagnetic waves. Surprisingly, the alliance of graphene and metamaterial provides a promising chance for THz applications which could bridge the 'THz gap' between the far-field and microwave region[15-16]. Recently, some researches about graphene metamaterial THz devices have been carried out. For instance, Alaee *et. al* proposed a perfect absorber by patterning graphene micro-ribbons on a dielectrics-metal layer[15], while Freitag *et. al* demonstrated a polarization sensitive gate tunable photodetector in the same way[16]. A modulator based on hybrid graphene/metamaterial structure was proposed by Han *et. al*, which can modulate the amplitude of THz waves up to 90%[17].

Among the THz applications, THz modulator is one of the most important devices. However, there are still some problems in current semiconductor-based modulators, such as poor modulation depth and strict temperature requirement[18]. Further improvements of performance are largely needed for practical THz applications. By patterning Split Ring Resonators (SRRs) arranged on a SiO_2 substrate, we demonstrate an active graphene metamaterial device which affords an efficient methodto modulate THz waves. The geometric parameters of the structure are $d=4$ μm (length of unit cell), $e=3$ μm (width of unit cell). The unit SRR resonatormade of graphene layer has a length of $c=2.8$ μm (width of the square ring), $b=3.6$ μm (length of the square ring), $a=1.2$ μm is the line-width of the arm, thickness of substrate layer and graphene is 105 nm and 1 nm, respectively. The gap distance in our simulation is a varied parameter, firstly, we assume that $g=0.5$ μm. By turning the Fermi level of graphene, the transmission of the graphene metamaterial can be dynamically modulated. By changing the gap distance in SRR, high modulation depth can be achieved in both higher and lower frequency region in our monolayer structure. Furthermore, the peak modulation depth can be further enhanced to 93% and 95% by stacking graphene layers, respectively. Our design may have potentials in the view of broadband THz optoelectronic devices, such as THz absorber, detector and modulator.

1 Design and theory

The periodic unit cells of the graphene metamaterial are shown in Fig. 1(a) and (b). The parameters are as aforementioned. The SRRs are periodically arranged on quartz substrate with the permittivity $\varepsilon=2.25$. We can ignore the influence of the substrate because of its tiny absorption and unvaried refractive index. CST microwavestudiois used to calculate theelectromagnetic response with frequency domain solver. In the calculation, unit cell boundary conditions are set in both X and Y directions, while open boundary condition is set in Z direction (Fig. 1(a)). The THz transverse electromagnetic wavepropagates in minus Z direction with the linear polarization alongthe X axis. The S-parameter S_{21} represents the coefficients of transmissions, the transmission can be expressed as $T=|S_{12}|^2$.

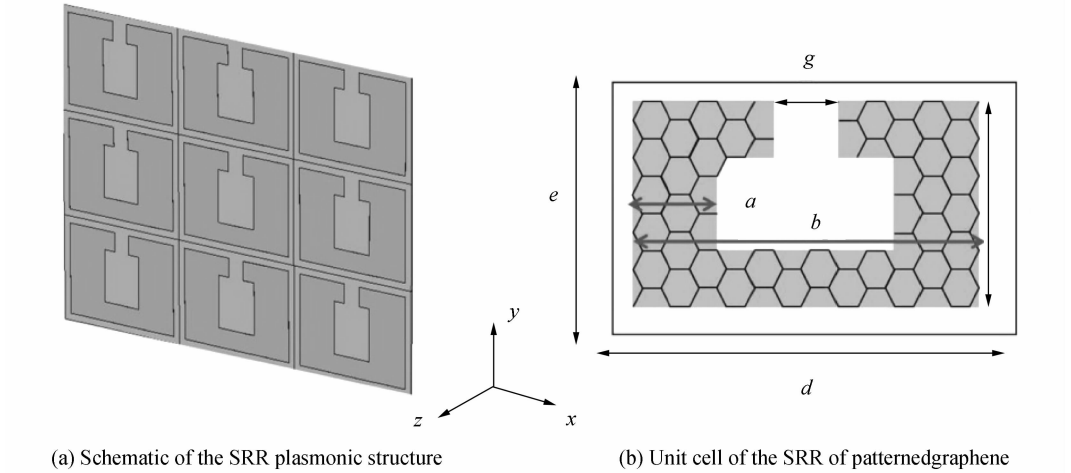

(a) Schematic of the SRR plasmonic structure (b) Unit cell of the SRR of patternedgraphene

Fig. 1 Design of the SRR of patternedgraphene

The conductivity of graphene includes both interband and intraband transition. The loss or absorption of electromagnetic waves is connected with imaginary part of the permittivity of graphene, thus it is proportional to the real part of optical conductivity[2], which can be described as[9-10]

$$\sigma(\omega)=\sigma_{\text{int}ra}(\omega)+\sigma_{\text{int}er}(\omega) \tag{1}$$

$$\sigma_{\text{int}ra}(\omega)=-\frac{\mathrm{i}e^2k_bT}{\pi\hbar^2(\omega+\mathrm{i}2\Gamma)}\left[E_F/(k_bT)+2\ln(1+e^{[-E_F/(k_bT)]})\right. \tag{2}$$

$$\sigma_{\text{int}er}(\omega)=-\frac{\mathrm{i}e^2}{4\pi\hbar}\ln\left(\frac{2E_F-(\omega+\mathrm{i}4\pi\Gamma)\hbar}{2E_F+(\omega+\mathrm{i}4\pi\Gamma)\hbar}\right) \tag{3}$$

where, ω is the angular frequency, e is the electron charge, $\hbar$ is the reduced Planck constant and K_b is Boltzmann's constant, T is the temperature, E_F is Fermi level which can be also described as μ (chemical potential), $\Gamma=E_F\mu_\nu/e\upsilon_F$ is scattering coefficient, $\upsilon_F\approx10^6$ m·s^{-1} is the Fermi velocity, $\mu_\nu=10\ 000$ cm^2·V^{-1}·s^{-1} mobility. The intraband transition dominates in THz region while interband transition dominatesthe visible-infrared region. Thus, the conductivity can be regarded as a Drude-model. The parameters are all constant except the Fermi energy E_F of graphene. It can be easily changed either by physical and chemical methods. Thus, the variation of E_F can efficiently influence the optical conductivity, which may further affect the electromagnetic response of graphene-based structures.

2 Different Fermi levels

We investigate the influences of Fermi level on the THz transmission. The THz transmission spectra of different Fermi level are shown in Fig. 2(a), where the transmission dips correspond to plasmon resonances. The three resonant modes appear at approximate $F_1=3.5$ THz, $F_2=10$ THz, and F_3 at 13.3 THz with E_F within 0.8 eV, respectively. We observe that with $E_F=0.8$ eV, there is a trend for F_3, but is beyond our calculation range. The amplitude in transmission spectra embodies the resonant strength. We can see that with $E_F=0$, the transmission is nearly to 1 compared to other Fermi levels. As Fig. 2(a) shown, the transmission of F_1 decreases from 0.63 to 0.35 with Fermi level increasing from 0.5 eV to 0.8 eV. The transmission of F_2 is decreased by 0.26 with increasing Fermi level. For F_3, the transmission from 0.55 to 0.45 with Fermi level from 0.5 to 0.6 eV. In other words, with the increasing of Fermi level, the resonant strength of the three modes increases dramatically, especially the magnetic resonance (F_1). What's more, the resonant frequencies of the three modes all demonstrate blue-shifts ($\Delta F_1=0.8$ THz, $\Delta F_2=1.4$ THz, $\Delta F_3=1.2$ THz) with increasing Fermi level. These phenomena can be expressed as the increasing carrier density. According to the formula $E_F=\hbar\upsilon_f\sqrt{\pi|n|}$, the carrier density gets to 4.68×10^{13} cm^{-2} with $E_F=0.8$ eV. Higher carrier concentration allows for stronger interaction between the incident wave and graphene plasmonic metamaterial. As such, higher carrier density yields to both stronger resonances strength and larger resonant frequencies. Fig. 2(b) shows the modulation depth as a function of frequency. The modulation depth can be defined as $1-T/T_0$, where T represents the minimal transmission (in our simulation, $E_F=0.8$ eV is where the Fermi level with minimal transmission) while T_0 represents the maximal transmission (0 eV). A peak modulation depth of 66% is observed at

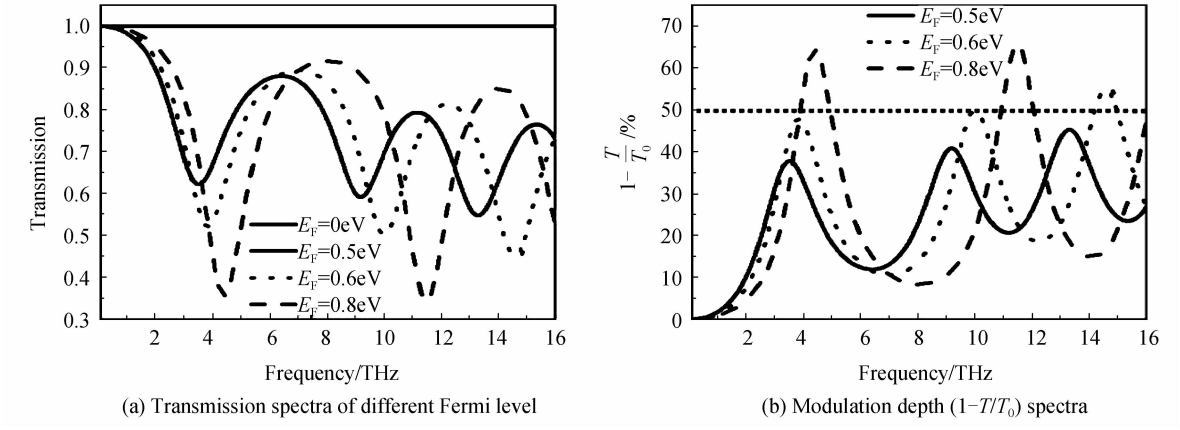

(a) Transmission spectra of different Fermi level (b) Modulation depth ($1-T/T_0$) spectra

Fig. 2 Transmission spectra and modulation depth ($1-T/T_0$) spectra of different Fermi level

11.5 THz with $E_F=0.8$ eV. Furthermore, at the resonant frequency of F_1, a modulation depth of 65% is also achieved with $E_F=0.8$ eV. Here, we define that an efficient modulation bandwidth is a bandwidth with modulation depth exceeding 50% (black dashed line). With $E_F=0.8$ eV, there are two modulation bandwidths (from 3.5 THz to 4 THz, 10.5 THz to 12 THz) results from F_1 and F_2, respectively. While one modulation bandwidth (13.8 THz to 14.6 THz) is achieved with F_3 with $E_F=0.6$ eV. These phenomena indicate that the proposed design perform well in modulating THz waves.

To further understand the mechanism of the resonant modes, we analyze the current distribution of the three modes. The surface current distributions of the resonant modes are shown in Fig. 3(a), (b) and (c). F_1 is one of the typical resonances of SRRs which can be explained as magnetic dipolar when the incident electric field is paralleled to the gap (along X-direction in Fig. 1). In this case, the electric field is polarized along X-axis, which is able to couple to the capacitance of SRR and induce a circulating current. Thus, this can lead to a magnetic resonance (LC resonance)[19-21]. The current distribution of F_2 is shown in Fig. 3(b) which can be explained as high order plasmonic mode. For F_2 is not a simple dipole mode, although the charge oscillates horizontally across the bottom of the arm, the opposite corners are in phase[22]. Thus, it can be described as a quadrupole mode. F_3 is also a high order plasmonic mode with current distribution shown in Fig. 3 (c) which is similar with F_2.

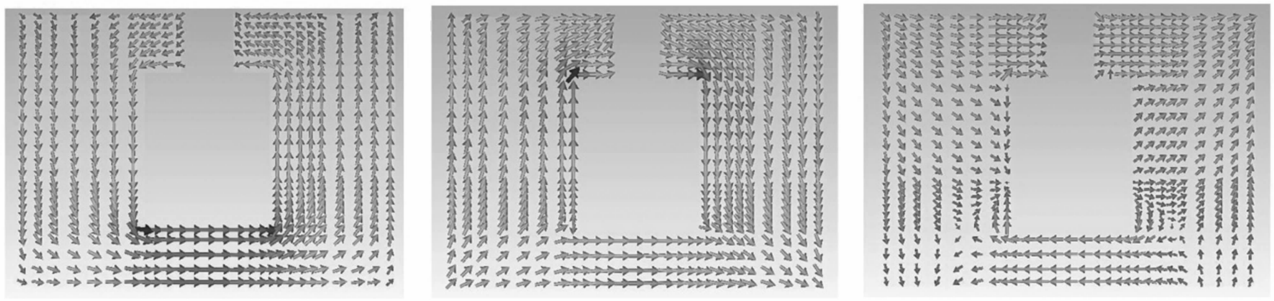

Fig. 3 Current distribution of the three resonant modes at $E_F=0.5$ eV

T represents the transmission of 0.8 eV and T_0 represents the transmission of 0 eV, the black dashed line represents the modulation depth of 50%.

3 Different gap distances

As the electric field couples to the capacitance of SRR, we investigated the influence of capacitance on the resonances. As such, we calculated the transmissions of different gap distance. Fig. 4(a) shows the transmission spectra of different gap distance (0.1 μm to 0.9 μm) at 0.8 eV. The spectra unambiguously show that there are three resonant modes with g less than 0.3 μm during our calculation range. With g greater than 0.3 μm and less than 0.9 μm, there are two resonant modes. The resonant strength of F_1 is increased with transmission of decreases from 0.46 to 0.32 with g increasing from 0.1 μm to 0.9 μm. The transmission of F_2 increases from 0.19 to 0.49 with increasing gap distance, which means the resonant strength of F_2 is decreased. What's more, resonant frequency of F_1 blue-shifts from 4 THz to 4.5 THz while F_2 blue-shifts from 10.4 THz to 11.6 THz with increasing g. The resonant frequency of inductance-capacitance (LC) can be described as $f=1/2\pi\sqrt{LC}$, where L represents the inductance while C represents the capacitance[10]. Obviously, with larger g the capacitance is surely decreased, which accounts for the blueshifts of F_1. Fig. 4(b) shows the modulation depth as a function of frequency. A peak modulation depth of 81% is achieved by this monolayer patterned graphene metamaterial with $g=0.1$ μm during higher frequency region (11 THz). Furthermore, a peak modulation depth of 68% is achieved with $g=0.9$ μm during lower frequency region. This peculiarity implies that the proposed design is efficient in modulating higher frequency THz waves with wider gap distance, while efficient in modulating lower frequency THz waves with narrower gap distance. Moreover, each gap distance has modulation bandwidth exceeding 50% both lower and higher frequency regions. With $g=0.1$ μm, the modulation bandwidth (2.6 THz) is the greatest which ranges from 3.8 to 4.2 THz and 9.2 to 11.4 THz. With $g=0.5$ μm,

although the peak modulation depths of two region are not the greatest, it is a proper candidate to modulate both high and low frequency region THz waves.

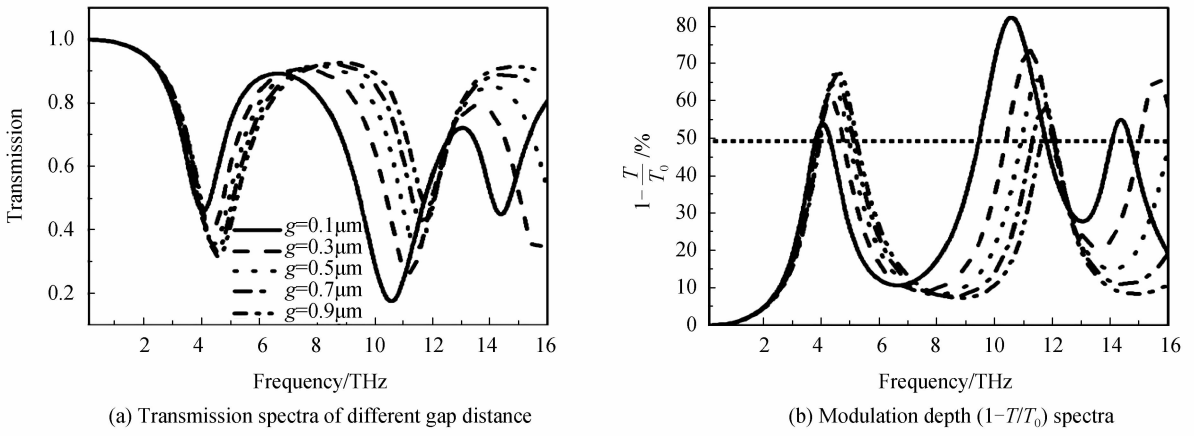

(a) Transmission spectra of different gap distance (b) Modulation depth ($1-T/T_0$) spectra

Fig. 4 Transmission spectra and modulation depth ($1-T/T_0$) spectra of different gap distance

4 Different graphene plasmonic metamaterial layers

In order to obtain more efficient THz modulation, we investigated the influence of stacked graphene plasmonic metamaterial layers on transmission and resonance. The gap distance here is 0.5 μm. Other parameters are the same as aforementioned monolayer structure. Fig. 5(a) shows the transmission spectra of graphene metamaterial when the number of graphene layers varies from double to five. The third resonant mode is out of our calculation range with garphene layers more than two. We observed two prominent features in Fig. 5(a). First, the resonance strengths of both F_1 and F_2 become stronger. The transmission of F_1 reduces to 0.05 with five graphene layers, while F_2 from 0.24 to 0.07 with layers from two to five. Second, the resonance frequency of stacked layers for F_1 blue-shifted from 6.2 to 9.8 THz while F_2 from 16.2 to 23.6 THz with layers changing from two to five. These phenomena in multiple graphene layers can be explained by the stronger Coulomb interaction of the adjacent layers[23-24]. The in-phase collective motion of carriers among the layers results in stronger restoring force due to dipole-dipole coupling[23]. Since the thickness of quartz between each layer of graphene SRRs is 1nm, which is much smaller than the unit cell. Our simulation can nicely satisfy the strong coupling condition[24]. The carrier density of each graphene layer is identical, in this assumption, the carrier density of stacked graphene plasmonic layers can be regarded as N times of the density in original monolayer graphene, where N is the number of graphene layers[24]. Fig. 5(b) shows the modulation depth spectra of multiple graphene layers. The peak modulation depth of five-layer graphene metamaterial approaches to 95%, and the modulation bandwidth is8 THz (7.8 to 11.8 THz and 21 to 25 THz). With the number of graphene layers increasing from one to five, the peak modulation depth increases to 95% in low frequency region while to 93% in high frequency . The modulation bandwidth enlarges from 2.6 to 8 THz. In summary , by stacking graphene

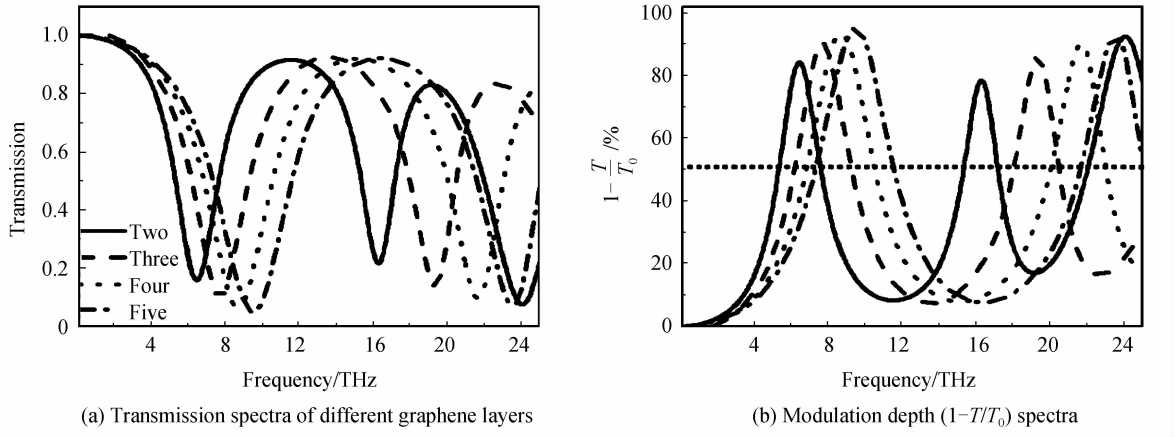

(a) Transmission spectra of different graphene layers (b) Modulation depth ($1-T/T_0$) spectra

Fig. 5 Transmission spectra and modulation depth ($1-T/T_0$) spectra of different graphene layers

layers, both in low frequency and high frequency region, not only great enhancement in modulation depth is achieved, but also the modulation bandwidth. It implies that by further increasing the graphene layers, the modulation depth and modulation bandwidth are able to be further improved. Our design shows great potentials in manipulating THz waves during a broad frequency range.

5 Conclusion

In summary, we propose a graphene-based metamaterial which can efficiently modulate the transmitted THz waves. It is revealed that by increasing the Fermi level, the resonant strength of the plasmonic modes can be enhanced, thus the enhancement of modulation. Furthermore, by changing the gap distance, a high modulation depth of 81% is achieved in higher frequency region, while 68% is achieved in lower frequency region by our monolayer graphene metamaterial structure. By further stacking graphene layers, the above value is promoted to 93% and 95%, respectively. Our design may have potential applications for THz andinfrared band graphene photonics and optoelectronics.

References

[1] SUN Zhi-pei, MARTINEZ A, WANG Feng. Optical modulators with 2D layered materials[J]. *Nature Photonics*, 2016, **10**(4): 227-238.

[2] SENSALE-RODRIGUEZ B, YAN Ru-sen, LIU Lei, *et al*. Graphene for reconfigurable terahertz optoelectronics[J]. *Proceedings of the IEEE*, 2013, **101**(7): 1705-1716.

[3] FANG Zhe-yu, THONGRATTANASIRI S, SCHLATHER A, *et al*. Gated tunability and hybridization of localized plasmons in nanostructured graphene[J]. *Acs Nano*, 2013, **7**(3): 2388-2395.

[4] LIU Ming, YIN Xiao-bo, ERICK U, *et al*. A graphene-based broadband optical modulator[J]. *Nature*, 2011, 4**74**(7349): 64-67.

[5] JIANG Man, Qi Mei, REN Zhao-yu, *et al*. A graphene Q-switched nanosecond Tm-doped fiber laser at 2 μm[J]. *Laser Physics Letters*, 2013, **10**(5): 79-83.

[6] SPIRITO D, COQUILLAT D, LOMBARDO A, *et al*. High performance bilayer-graphene terahertz detectors[J]. *Applied Physics Letters*, 2013, **104**(6): 061111.

[7] QIN Shi-qiao, ZHU Z H, GUO C C, *et al*. Electrically tunable polarizer based on anisotropic absorption of graphene ribbons[J]. *Applied Physics A Materials Science & Processing*, 2014, **114**(4): 1017-1021.

[8] WEIS P, REINHARD B, BRODYANSKI A, *et al*. Spectrally wide-band terahertz wave modulator based on optically tuned graphene.[J]. *Acs Nano*, 2012, **6**(10): 9118-9124.

[9] SENSALE-RODRIGUEZ B, FANG Tian, YAN Ru-sen, *et al*. Unique prospects for graphene-based terahertz modulators [J]. *Applied Physics Letters*, 2011, **99**(11): 113104.

[10] LI Jia-yuan, REN Zhao-yu, XU Xin-long *et al*. Graphene – metamaterial hybridization for enhanced terahertz response [J]. *Carbon*, 2014, **78**(18): 102-112.

[11] SENSALE-RODRIGUEZ B, FANG Tian, YAN Ru-sen, *et al*. Broadband graphene terahertz modulators enabled by intraband transitions[J]. *Nature Communications*, 2012, **3**(1): 85-100.

[12] LIU Na, HARALD G. Coupling effects in optical metamaterials[J]. *Angewandte Chemie International Edition*, 2010, **49**(51): 9838-9852.

[13] BERARDI S R, RAFIQUE S, YAN Ru-sen, *et al*. Terahertz imaging employing graphene modulator arrays[J]. *Optics Express*, 2013, **21**(2): 2324-2330.

[14] ANDRYIEUSKI A, LAVRINENKOA. V. Graphenemetamaterials based tunable terahertz absorber: effective surface conductivity approach[J]. *Optics Express*, 2013, **21**(7): 9144-9155.

[15] ALAEE R, MOHAMED F, CARSTEN R, *et al*. A perfect absorber made of a graphene micro-ribbon metamaterial[J]. *Optics Express*, 2012, **20**(27): 28017-28024.

[16] FREITAG M, TONY L, ZHU Wen-juan, *et al*. Photocurrent in graphene harnessed by tunable intrinsic plasmons[J]. *Nature Communications*, 2013, **4**(3): 131-140.

[17] LEE S H, LIU Ming, ZHANG Xiang, *et al*. Switching terahertz waves with gate-controlled active graphene metamaterials[J]. *Nature Materials*, 2012, **11**(11): 936-941.

[18] HAN Jian-guang, ZHANG Wei-li, GU Jian-qiang, *et al*. Broadband resonant terahertz transmission in a composite metal-dielectric structure[J]. *Optics Express*, 2009, **17**(19): 16527-16534.

[19] ENKRICH C, WEGENER M, LINDENS, *et al*. Magnetic metamaterials at telecommunication and visible frequencies [J]. *Physical Review Letters*, 2005, **95**(20): 1168-1174.

[20] PADILLA W J, TAYLOR A J, HIGHSTRETE C, *et al*. Dynamical electric and magnetic metamaterial response at terahertz frequencies[J]. *Conference on Lasers & Electro-optics*, 2008, **96**(10): 1-2.

[21] SERSIC I, FRIMMER M, VERHAGEN E, *et al*. Electric and magnetic dipole coupling in near-infrared split-ring metamaterial arrays[J]. *Physical Review Letters*, 2009, **103**(21): 213902

[22] CORRIGAN T D, KOLB P W, SUSHKOVA. B, *et al*. Optical plasmonic resonances in split-ring resonator structures: An improved LC model[J]. *Optics Express*, 2008, **16**(24): 19850-19864.

[23] YAN Hu-gen, XIA Feng-nian, CHANDRAB, *et al*. Tunable infrared plasmonic devices using graphene/insulator stacks [J]. *Nature Nanotechnology*, 2012, **7**(5): 330-334.

[24] YAO Ze-han, HUANG Yuan-yuan, WANG Qian, *et al*. Tunable surface-plasmon-polariton-like modes based on graphene metamaterials in terahertz region[J]. *Computational Materials Science*, 2015, **117**: 544-548.